

Sparsification as a Remedy for Staleness in Distributed Asynchronous SGD

Rosa Candela Giulio Franzese Maurizio Filippone Pietro Michiardi

Abstract

Large scale machine learning is increasingly relying on distributed optimization, whereby several machines contribute to the training process of a statistical model. While there exist a large literature on stochastic gradient descent (SGD) and variants, the study of countermeasures to mitigate problems arising in asynchronous distributed settings are still in their infancy. The key question of this work is whether sparsification, a technique predominantly used to reduce communication overheads, can also mitigate the staleness problem that affects asynchronous SGD. We study the role of sparsification both theoretically and empirically. Our theory indicates that, in an asynchronous, non-convex setting, the ergodic convergence rate of sparsified SGD matches the known result $\mathcal{O}(1/\sqrt{T})$ of non-convex SGD. We then carry out an empirical study to complement our theory and show that, in practice, sparsification consistently improves over vanilla SGD and current alternatives to mitigate the effects of staleness.

1 Introduction

The analysis of Stochastic Gradient Descent (SGD) (Robbins and Monro, 1951) and its variants (see (Bottou et al., 2018) for an overview) has received a lot of attention recently, due to its popularity as an optimization algorithm in machine learning. SGD addresses the computational bottleneck of gradient descent, as the computation of a stochastic gradient is cheaper than that of a full gradient. SGD trades a larger number of iterations to converge for a cheaper cost per iteration. The *mini-batch* variant of SGD allows to control the number and the cost per iteration, making it the prime choice for optimization in deep learning (Bottou, 2010; Bottou et al., 2018).

We consider the problem of optimizing the d -dimensional parameters $\mathbf{x} \in \mathbb{R}^d$ of a model and its associated finite-sum *non-convex* loss function $f(\mathbf{x}) = \frac{1}{n} \sum_{i=1}^n f(\mathbf{x}, i)$, where $f(\mathbf{x}, i)$ $i = 1, \dots, n$ is the loss function for a single training sample i . SGD iterations have the following form:

$$\mathbf{x}_{t+1} = \mathbf{x}_t - \eta_t \mathbf{g}(\mathbf{x}_t, i),$$

where $\mathbf{x}_t, \mathbf{x}_{t+1} \in \mathbb{R}^d$ are the model iterates, $\eta_t > 0$ is the learning rate/step size and $\mathbf{g}(\mathbf{x}_t, i) = \nabla f(\mathbf{x}_t, i)$ is a stochastic gradient.

In this work, we are interested in the increasingly popular distributed setting, whereby SGD runs across several machines, which contribute to the model updates \mathbf{x}_{t+1} by computing stochastic gradients of the loss using locally available training data (Dean et al., 2012; Ho et al., 2013; Chilimbi et al., 2014; Li et al., 2014; Jiang et al., 2017). The analysis of the convergence behavior of SGD, both in synchronous (Chen et al., 2016; Zhang et al., 2016; Bottou et al., 2018) and asynchronous (Recht et al., 2011; De Sa et al., 2015; Lian et al., 2015; Liu and Wright, 2015; Bottou et al., 2018) settings has been widely studied in the literature. In this work, we focus on the asynchronous setting, which is particularly challenging because distributed workers might produce gradient updates for a loss computed on *stale* versions of the current model iterates (Ho et al., 2013; Damaskinos et al., 2018; Lin et al., 2018; Dutta et al., 2018; Dai et al., 2019).

In this context, communication overheads have been considered as a key issue to address, and a large number of works have been proposed to mitigate such overheads (Stich, 2019; Yu et al., 2019; Wangni et al., 2018; Alistarh et al., 2017; Wen et al., 2017; Aji and Heafield, 2017; Dryden et al., 2016). In particular, sparsification methods (Stich et al., 2018; Alistarh et al., 2018; Wangni et al., 2018) have achieved remarkable results, albeit for synchronous setups. The key idea is to apply smaller and more efficient gradient updates, by applying a sparsification operator to the stochastic gradient, which results in updates of size $k \ll d$.

In this work, we also consider sparsification methods, but *instead of focusing on communication overheads, we study the potential benefits of sparsification to alleviate the negative effects of staleness*. For the first time, we provide a concise and simple convergence rate analysis for sparsified SGD in a distributed, *asynchronous* setting, and show that it converges at the same rate of standard SGD in the same setup. We attribute this result to the particular kind of sparsification operator we study, namely the top- k operator, which contributes to producing “coherent” gradient updates even when these are computed on stale models. Our extensive empirical analysis of sparsified SGD, which we also compare against alternative techniques to cope with staleness from the recent literature, complements our theory. We show that, in practice, sparsification induces faster convergence, in the sense that the number of iterations required to reach a target accuracy level are smaller than standard SGD and alternatives.

1.1 Related work

The analysis of SGD (Robbins and Monro, 1951) and its convergence properties has recently attracted a lot of attention, especially in the field of machine learning (Bottou et al., 2018; Moulines and Bach, 2011), where SGD is considered the workhorse optimization method. Large scale models and massive datasets have motivated researchers to focus on distributed machine learning, whereby multiple machines compute stochastic gradients using partitions of the dataset and a parameter server maintains a globally shared model.

Asynchronous systems (Recht et al., 2011; Dean et al., 2012; Li et al., 2014;

Chilimbi et al., 2014) provide fast model updates, but the use of stale parameters affects convergence speed. One way to reduce the staleness effect is to give a smaller weight to stale updates. In (Jiang et al., 2017; Damaskinos et al., 2018) gradient contributions are dampened through a dynamic learning rate. Stale-synchronous parallel (SSP) models (Ho et al., 2013; Damaskinos et al., 2018) limit instead the maximum staleness, discarding updates that are too “old”. Interestingly, the work in (Mitliagkas et al., 2016), suggests to view staleness as a form of implicit momentum, and study, under a simple model, how to adjust explicit, algorithmic momentum to counterbalance the effects of staleness.

Synchronous systems (Chen et al., 2016) guarantee higher statistical efficiency, but the presence of stragglers slows down the learning algorithm. One solution is provided by the so called local SGD models (Lin et al., 2018; Stich, 2019; Yu et al., 2019), which reduce the synchronization frequency by allowing nodes to compute local model parameters, which are averaged in a global model update. A second family of approaches seeks to improve synchronous systems by reducing the cost of communicating gradients upon every iteration. Quantization techniques reduce the number of bits to represent the gradients before communication (Seide et al., 2014; Alistarh et al., 2017; Wen et al., 2017), sparsification methods select a subset of the gradient components to communicate (Aji and Heafield, 2017; Dryden et al., 2016; Strom, 2015; Stich et al., 2018; Alistarh et al., 2018), and loss-less methods use large mini-batches to increase the computation-communication ratio (Goyal et al., 2017; You et al., 2017).

Recently it has been noted that sparsification techniques can be a promising approach to improve the performance of SGD in asynchronous, distributed settings (Alistarh et al., 2018), but no theoretical analysis nor experimental study has confirmed it yet. In this work, for the first time, we provide a theoretical and empirical analysis on the benefits of gradient sparsification in mitigating the effects of stale updates, which represent the main challenge in asynchronous settings.

1.2 Contributions

We study finite-sum non-convex optimization of loss functions of the form $f(\mathbf{x}) : \mathbb{R}^d \rightarrow \mathbb{R}$, and assume that f is continuously differentiable and bounded below, that $\nabla f(\mathbf{x})$ is L -Lipschitz smooth, that the variance of the stochastic gradient is bounded, and that the staleness induced by asynchrony is also bounded. We analyze a mini-batch asynchronous SGD algorithm and apply a sparsification operator $\Phi_k[\mathbf{g}(\mathbf{x}_{\tau_t}, \xi_t)]$ with $k \ll d$, that can be coupled with an error correction technique, often called *memory* (Stich et al., 2018).

We prove ergodic convergence of the gradient of $f(\mathbf{x})$, for an appropriately chosen learning rate. In particular, we focus on memory-less variants, which are simpler to analyze, and show that asynchronous sparsified SGD converges at the same rate as standard SGD.

In this paper, the main theoretical contribution is as follows. Let the sparsifi-

cation coefficient be $\rho = k/d$. Then, it holds that:

$$\min_{0 \leq t \leq T} \mathbb{E} \left[\|\nabla f(\mathbf{x}_t)\|^2 \right] \leq \frac{\left(\sum_{t=0}^{T-1} \left(\frac{\eta_t^2 L}{2} \sigma^2 \right) \right) + \Lambda + C}{\sum_{t=0}^{T-1} \left(\eta_t \rho \mu - \frac{\eta_t^2 L}{2} \right)},$$

where $\Lambda = f(\mathbf{x}_0) - \inf_{\mathbf{x}} f(\mathbf{x})$ and C, μ are finite positive constants (whose role will be clarified later). In particular for a suitable constant learning rate $\eta_t = \eta = \frac{\rho \mu}{L \sqrt{T}}$ we can derive as a corollary that:

$$\min_{0 \leq t \leq T} \mathbb{E} \left[\|\nabla f(\mathbf{x}_t)\|^2 \right] \leq \left(\frac{\sigma^2}{2} + \frac{(\Lambda + C)L}{(\rho \mu)^2} \right) \frac{1}{\sqrt{T}},$$

up to a negligible approximation for large T (details in the supplement).

We define sparsified SGD formally in Section 2, both in its memory and memory-less variants, and outline our proof for the memory-less case in Section 2.5. In Section 3 we provide an extensive empirical study of the convergence behavior of the two variants of sparsified SGD and compare them to alternative approaches that address the staleness issue in asynchronous distributed settings. We complement our analysis with empirical evidence showing that sparsification induces faster convergence speeds, mitigating the effects staleness. Although we do not provide convergence guarantees for sparsified SGD with memory, our empirical results indicate that error correction dramatically improves the convergence properties of the algorithm, even in an asynchronous setting. Since it was missing in the literature, we conceived a powerful open-source simulator that allows a wide range of system architectures and configurations to study SGD and its variants.

2 Sparsified Asynchronous SGD

In this Section we define two variants of sparsified SGD algorithms, with and without error correction, and emphasize the role of model staleness induced by the distributed, asynchronous setup we consider. We provide convergence results for the memory-less version, and overview our proof strategy.

2.1 Distributed, asynchronous configuration

The standard way to scale SGD to multiple computing nodes is via *data-parallelism*: a given set of worker machines have access to the n training samples through a distributed filesystem. Workers process samples concurrently: each node receives a copy of the parameter vector \mathbf{x}_t , and computes stochastic gradients locally. Then, they send their gradients to a parameter server (PS). Upon receiving a gradient from a worker, the PS updates the model by producing a new iterate \mathbf{x}_{t+1} .

Due to asynchrony, a computing node may use a *stale* version of the parameter vector: for example, a worker may compute the gradient of $f(\mathbf{x}_{\tau_t})$, $\tau_t \leq t$ and

send it to the PS that will use it to update the more recent model \mathbf{x}_t . We call τ_t the *staleness of a gradient update*. As stated more formally in Section 2.4, in this work we assume **bounded staleness**, which is realistic in the setup we consider. Other works, e.g. that consider Byzantine attackers (Damaskinos et al., 2018), drop this assumption.

2.2 Gradient sparsification

We begin by defining the sparsification operator we consider in this work. A variety of compression (Bernstein et al., 2018a,b), quantization (Dryden et al., 2016; Alistarh et al., 2017) and sparsification (Alistarh et al., 2018; Stich et al., 2018) operators have been considered in the literature. Here we use sparsification, albeit from an unusual perspective: instead of reducing communication overheads, we are interested in the role of sparsification in mitigating the problem of staleness.

Definition 2.1. *Given a vector $\mathbf{u} \in \mathbb{R}^d$, a parameter $1 \leq k \leq d$, the operator $\Phi_k(\mathbf{u}) : \mathbb{R}^d \rightarrow \mathbb{R}^d$ is defined as:*

$$(\Phi_k(\mathbf{u}))_i = \begin{cases} (\mathbf{u})_{\pi(i)}, & \text{if } i \leq k, \\ 0, & \text{otherwise} \end{cases}$$

where π is a permutation of the indices $[d]$ such that $(|\mathbf{u}|)_{\pi(i)} \geq (|\mathbf{u}|)_{\pi(i+1)}, \forall i \in 1, \dots, d$.

Essentially, $\Phi_k(\cdot)$ sorts vector elements by their magnitude, and keeps only the top- k . A key property of the operator we consider is called the k -contraction property (Stich et al., 2018), which we use in our convergence proofs. Note that our proof strategy holds also for randomized sparsification, which we do not study in this work.

Definition 2.2. *For a parameter $1 \leq k \leq d$, a k -contraction operator $\Phi_k(\mathbf{u}) : \mathbb{R}^d \rightarrow \mathbb{R}^d$ satisfies the following contraction property:*

$$\mathbb{E} \|\mathbf{u} - \Phi_k(\mathbf{u})\|^2 \leq \left(1 - \frac{k}{d}\right) \|\mathbf{u}\|^2.$$

Both the top- k operator we consider, and randomized variants, satisfy the k -contraction property (Alistarh et al., 2018; Stich et al., 2018). Next, we state a Lemma that we will use for our convergence rate results.

Lemma 2.1. *Given a vector $\mathbf{u} \in \mathbb{R}^d$, a parameter $1 \leq k \leq d$, and the top- k operator $\Phi_k(\mathbf{u}) : \mathbb{R}^d \rightarrow \mathbb{R}^d$ introduced in Definition 2.1, we have that:*

$$\|\Phi_k(\mathbf{u})\|^2 \geq \frac{k}{d} \|\mathbf{u}\|^2.$$

The proof of Lemma 2.1 uses the k -contraction property in Definition 2.2, as shown in Appendix A.1.

2.3 Memory and memory-less sparsified asynchronous SGD

We define two variants of sparsified SGD: the first uses sparsified stochastic gradient updates directly, whereas the second uses an error correction technique which accumulates information suppressed by sparsification. Since we consider an asynchronous, *mini-batch* version of SGD, additional specifications are in order.

Definition 2.3. *Given n training samples, let ξ_t be a set of indices sampled uniformly at random from $\{1, \dots, n\}$, with cardinality $|\xi_t|$. Let τ_t be the bounded staleness induced by the asynchronous setup, with respect to the current iterate t . That is, $t - S \leq \tau_t \leq t$. A stale, mini-batch stochastic gradient is defined as:*

$$\mathbf{g}(\mathbf{x}_{\tau_t}, \xi_t) = \frac{1}{|\xi_t|} \sum_{i \in \xi_t} \nabla f(\mathbf{x}_{\tau_t}, i).$$

Memory-less sparsified SGD. Given the operator $\Phi_k(\cdot)$, the memory-less, asynchronous sparsified SGD algorithm amounts to the following:

$$\mathbf{x}_{t+1} = \mathbf{x}_t - \eta_t \Phi_k(\mathbf{g}(\mathbf{x}_{\tau_t}, \xi_t)),$$

where $\{\eta_t\}_{t \geq 0}$ denotes a sequence of learning rates.

Sparsified SGD with memory. Given the operator $\Phi_k(\cdot)$, the asynchronous sparsified SGD with memory algorithm is defined as:

$$\begin{aligned} \mathbf{x}_{t+1} &= \mathbf{x}_t - \eta_t \Phi_k(\mathbf{m}_t + \mathbf{g}(\mathbf{x}_{\tau_t}, \xi_t)), \\ \mathbf{m}_{t+1} &= \mathbf{m}_t + \mathbf{g}(\mathbf{x}_{\tau_t}, \xi_t) - \Phi_k(\mathbf{m}_t + \mathbf{g}(\mathbf{x}_{\tau_t}, \xi_t)), \end{aligned}$$

where $\{\eta_t\}_{t \geq 0}$ denotes a sequence of learning rates, and \mathbf{m}_t represents the memory vector that accumulates the elements of the stochastic gradient that have been suppressed by the operator $\Phi_k(\cdot)$.

2.4 Ergodic convergence

Concerning the theoretical aspect of this work, we study convergence only for the memory-less variant of SGD. The convergence of sparsified SGD with memory has been studied for both strongly convex (Stich et al., 2018; Alistarh et al., 2018) and non-convex objectives (Alistarh et al., 2018), but only in the synchronous case. We thus focus on the analysis of the memory-less variant of sparsified SGD, as our goal is to understand if sparsification can mitigate staleness. Nevertheless, in our empirical study, we compare both variants, and verify that the one with memory considerably benefits from error correction, as expected (Stich et al., 2018).

Before proceeding with the statement of the main theorem, we formalize our assumptions:

Assumption 1. $f(\mathbf{x})$ is continuously differentiable and bounded below: $\inf_{\mathbf{x}} f(\mathbf{x}) > -\infty$.

Assumption 2. $\nabla f(\mathbf{x})$ is L -Lipschitz smooth:

$$\forall \mathbf{x}, \mathbf{y} \in \mathbb{R}^d, \|\nabla f(\mathbf{x}) - \nabla f(\mathbf{y})\| \leq L \|\mathbf{x} - \mathbf{y}\|.$$

Assumption 3. The variance of the (mini-batch) stochastic gradients is bounded:

$$\mathbb{E} \left[\|\mathbf{g}(\mathbf{x}_t, \xi_t) - \nabla f(\mathbf{x}_t)\|^2 \right] \leq \sigma^2,$$

where $\sigma^2 > 0$ is a constant.

Assumption 4. Distributed workers might use stale models to compute gradients $\mathbf{g}(\mathbf{x}_{\tau_t}, \xi_t)$. We assume bounded staleness, that is: $t - S \leq \tau_t \leq t$. In other words, the model staleness τ_t satisfies the inequality $t - \tau_t \leq S$. We call $S \geq 0$ the maximum delay.

Assumption 5. Let the *expected cosine distance* be:

$$\frac{\mathbb{E} [\langle \Phi_k(\mathbf{g}(\mathbf{x}_{\tau_t}, \xi_t)), \nabla f(\mathbf{x}_t) \rangle]}{\mathbb{E} [\|\Phi_k(\mathbf{g}(\mathbf{x}_{\tau_t}, \xi_t))\| \|\nabla f(\mathbf{x}_t)\|]} = \mu_t \geq \mu.$$

We assume, similarly to previous work (Dai et al., 2019), that the constant $\mu > 0$ measures the minimum discrepancy between the sparsified stochastic gradient and the full gradient.

Theorem 2.1. Let Assumptions 1–5 hold. Consider the memory-less variant of sparsified SGD defined in Section 2.3, which uses the $\Phi_k(\cdot)$ top- k sparsification operator for a given $1 \leq k \leq d$, defined in Definition 2.1. Then, for an appropriately defined learning rate $\eta_t = \frac{\rho\mu}{L\sqrt{t+1}}$ and for $\Lambda = \left(f(\mathbf{x}_0) - \inf_{\mathbf{x}} f(\mathbf{x}) \right)$, it holds that:

$$\min_{0 \leq t \leq T} \mathbb{E} \left[\|\nabla f(\mathbf{x}_t)\|^2 \right] \leq \frac{\left(\sum_{t=0}^{T-1} \left(\frac{\eta_t^2 L}{2} \sigma^2 \right) \right) + \Lambda + C}{\sum_{t=0}^{T-1} \left(\eta_t \rho \mu - \frac{\eta_t^2 L}{2} \right)}.$$

Corollary 2.1. Let the conditions of 2.1 hold. Then for an appropriately defined constant learning rate $\eta_t = \eta = \frac{\rho\mu}{L\sqrt{T}}$, we have that:

$$\min_{0 \leq t \leq T} \mathbb{E} \left[\|\nabla f(\mathbf{x}_t)\|^2 \right] \leq \left(\frac{\sigma^2}{2} + \frac{(\Lambda + C)L}{(\rho\mu)^2} \right) \frac{1}{\sqrt{T} - \frac{1}{2}}.$$

When $T \rightarrow \infty$ we can approximate $\sqrt{T} - \frac{1}{2} \simeq \sqrt{T}$.

Asymptotically, the convergence rate of memory-less sparsified SGD behaves as $\mathcal{O}\left(\frac{1}{\sqrt{T}}\right)$, which matches the best known results for non-convex SGD (Ghadimi and Lan, 2013), and for non-convex asynchronous SGD (Lian et al., 2015). Note that interpreting the constant learning rate is intuitive: the larger is ρ ,

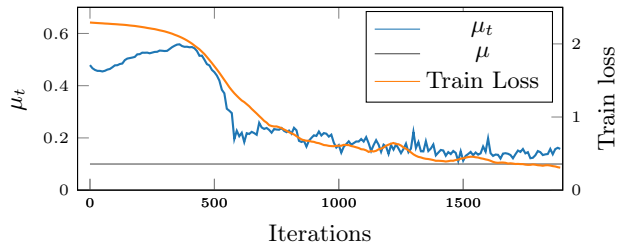


Figure 1: Empirical evaluation of Assumption 5: expected cosine similarity μ_t between sparsified and full gradients and training loss, as a function of algorithmic progress. Results for L1NET on MNIST to reach an accuracy of 91%; communication delays exponentially distributed with rate $\lambda = 0.1$; sparsified SGD with memory, using a coefficient $\rho = 10\%$.

i.e., gradients are not heavily sparsified, the larger we can set the learning rate; similarly, the larger is μ , i.e., the larger is the similarity between stale, sparse stochastic gradients and full gradients, the larger we can set the learning rate. Instead, it is more difficult to quantify the role of the constant terms in Corollary 2.1, especially those involving sparsification. While it is evident that aggressive sparsification (extremely small ρ) reduces convergence speed, the exact role of the second constant term heavily depends on the initialization and the geometry of the loss function, which we do not address in this work.

Remarks. A careful assessment of Assumption 5 is in order. We assume that a sparse version of a stochastic gradient computed with respect to a stale model, does not diverge too much from the true, full gradient.¹ We measure this coherency through a positive constant $\mu > 0$. However, it is plausible to question the validity of such assumption, especially in a situation where either the sparsification is too aggressive, or the maximum delay is too high. Note that previous work (Damaskinos et al., 2018) address the extreme case of unbounded staleness, which we do not study in our work. In those cases, a good approach is that of discarding stale contributions to model updates. Our experiments, instead, indicate that when staleness is bounded, such a mechanism is too aggressive, and harms the performance of SGD.

We have studied the limits of our assumption empirically, and report in Figure 1 the evolution of the expected cosine similarity μ_t defined in Assumption 5, as a function of algorithmic progress. Figure 1 also reports the training loss as a function of algorithmic progress. Our experiments indicate, as known from the SGD literature (Shwartz-Ziv and Tishby, 2017; Mandt et al., 2017; Saxe et al., 2018), that sparsified SGD evolves according to three regimes: a warm up phase, a steady progress toward a local minimum, and a “sampling” behavior around the local minimum, due to the constant learning rate. The expected cosine similarity μ_t mimics these three regimes: gradient coherency increases

¹A similar remark, albeit without sparsification, has been made in (Dai et al., 2019).

steadily until it drops when SGD arrives in its “sampling” phase, and it is always larger than a constant $0 < \mu < 1$.

While our results are in line with previous works (Stich et al., 2018; Dai et al., 2019), in this work we can only claim that sparsification doesn’t hurt the asymptotic convergence rate, not that it improves it. As a consequence, in this paper, we resort to an empirical validation to further investigate the role of sparsification in alleviating the impact of staleness.

2.5 Proof Sketch

We now give an outline of the proof, whereas the full proof is available in Appendix A. Following standard practice in non-convex asynchronous settings (Liu and Wright, 2015; Lian et al., 2015), we settle for a weaker notion of convergence, namely showing that the memory-less, sparsified asynchronous SGD algorithm converges ergodically to a local minimum of the function f . Our strategy is to bound the expected sum-of-squares gradients of f .

By the L -Lipshitz property of $\nabla f(x)$ (see Assumption 2), we have that:

$$\begin{aligned} f(\mathbf{x}_{t+1}) &\leq f(\mathbf{x}_t) + \langle \mathbf{x}_{t+1} - \mathbf{x}_t, \nabla f(\mathbf{x}_t) \rangle + \\ &\quad + \frac{L}{2} \|\mathbf{x}_{t+1} - \mathbf{x}_t\|^2 \\ &= f(\mathbf{x}_t) - \eta_t \langle \Phi_k[\mathbf{g}(\mathbf{x}_{\tau_t}, \xi_t)], \nabla f(\mathbf{x}_t) \rangle \\ &\quad + \frac{\eta_t^2 L}{2} \|\Phi_k[\mathbf{g}(\mathbf{x}_{\tau_t}, \xi_t)]\|^2. \end{aligned} \tag{1}$$

The strategy to continue the proof is to find an upper bound for the term $\mathbb{E} \left[\|\Phi_k[\mathbf{g}(\mathbf{x}_{\tau_t}, \xi_t)]\|^2 \right]$ and a lower bound for the term $\mathbb{E} [\langle \Phi_k[\mathbf{g}(\mathbf{x}_{\tau_t}, \xi_t)], \nabla f(\mathbf{x}_t) \rangle]$.

Let’s focus on the term $\eta_t \langle \Phi_k[\mathbf{g}(\mathbf{x}_{\tau_t}, \xi_t)], \nabla f(\mathbf{x}_t) \rangle$. Using Lemma 2.1, and Assumption 5, and algebraic manipulations, we can bound the expectation of the above term as follows:

$$\mathbb{E} [\eta_t \langle \Phi_k[\mathbf{g}(\mathbf{x}_{\tau_t}, \xi_t)], \nabla f(\mathbf{x}_t) \rangle] \geq \eta_t \rho \mu \mathbb{E} [\|\nabla f(\mathbf{x}_t)\|^2],$$

where $\rho = k/d$, and μ is defined in Assumption 5.

Next, we can bound the expectation of the term $\frac{\eta_t^2 L}{2} \|\Phi_k[\mathbf{g}(\mathbf{x}_{\tau_t}, \xi_t)]\|^2$ by remarking that:

$$\mathbb{E} \left[\|\Phi_k[\mathbf{g}(\mathbf{x}_{\tau_t}, \xi_t)]\|^2 \right] \leq \mathbb{E} \left[\|\nabla f(\mathbf{x}_{\tau_t})\|^2 \right] + \sigma^2.$$

We then introduce a bound for the term:

$$\sum_{t=0}^{T-1} \eta_t^2 \mathbb{E} \left[\|\nabla f(\mathbf{x}_{\tau_t})\|^2 \right] \leq \sum_{t=0}^{T-1} \eta_t^2 \mathbb{E} \left[\|\nabla f(\mathbf{x}_t)\|^2 \right] + C,$$

where C is a positive finite constant.

Finally, if we take the expectation of the whole inequality 1, sum over t from 0 to $T - 1$, use Assumption 1 and Assumption 5, the derivations above, and let $\Lambda = \left(f(\mathbf{x}_0) - \inf_{\mathbf{x}} f(\mathbf{x}) \right)$, by rearranging we obtain:

$$\sum_{t=0}^{T-1} \left(\eta_t \rho \mu - \frac{L \eta_t^2}{2} \right) \mathbb{E} \left[\|\nabla f(\mathbf{x}_t)\|^2 \right] \leq \Lambda + C + \frac{\sigma^2 L}{2} \sum_{t=0}^{T-1} \eta_t^2.$$

from which we derive the result of Theorem 2.1:

$$\min_{0 \leq t \leq T} \mathbb{E} \left[\|\nabla f(\mathbf{x}_t)\|^2 \right] \leq \frac{\left(\sum_{t=0}^{T-1} \left(\frac{\eta_t^2 L}{2} \sigma^2 \right) \right) + \Lambda + C}{\sum_{t=0}^{T-1} \left(\eta_t \rho \mu - \frac{\eta_t^2 L}{2} \right)}.$$

Moreover, by choosing an appropriate constant learning rate ($\eta_t = \frac{\rho \mu}{L \sqrt{T}}$), we can derive Corollary 2.1:

$$\min_{0 \leq t \leq T} \mathbb{E} \left[\|\nabla f(\mathbf{x}_t)\|^2 \right] \leq \left(\frac{\sigma^2}{2} + \frac{(\Lambda + C)L}{(\rho \mu)^2} \right) \frac{1}{\sqrt{T} - \frac{1}{2}}.$$

3 Experiments

Our goal is to compare, empirically, recent alternatives to mitigate the effects of staleness in asynchronous distributed optimization. Whereas the benefits of sparsification have been extensively validated in the literature (Aji and Heafield, 2017; Dryden et al., 2016; Seide et al., 2014; Strom, 2015; Alistarh et al., 2017), such works focus on communication costs in a synchronous setup, with the exception of the work in (Stich et al., 2018), which illustrates a simple experiment in a multi-core asynchronous setup. Instead, our experiments focus on supporting our claims and analysis by measuring the benefits of sparsification in distributed scenarios with increasing staleness levels.

For our experimental campaign, we have built a custom simulator that plugs into existing machine learning libraries to leverage automatic differentiation and the vast availability of models, but abstracts away the complications of a real distributed setting. With this setup, it is easy to compare a variety of stochastic optimization algorithms on realistic and complex loss functions. More details about our simulator are given in Appendix C.

3.1 Experimental setup

SGD variants. We compare sparsified SGD without (ϕ SGD) and with memory (ϕ MEMSGD) to the following alternatives: “vanilla” asynchronous SGD (ASGD) and KARDAM (Damaskinos et al., 2018), which was conceived to combat staleness, in addition to Byzantine faults, using a dampening factor to weight gradient contributions based on their staleness level. For all algorithms, and for all staleness scenarios, we perform a grid search to find the best learning

rate. For KARDAM, we use the same configuration for the dampening function as in (Damaskinos et al., 2018). We also studied LocalSGD (Stich, 2019), which advocates for occasional model averaging while letting worker machines progress independently, but do not include it in our results due to its sub-par performance.

When relevant, Figures report error bars using standard deviation, obtained by repeating our experiments 5 times. Note that for direct comparisons on individual experiments to be fair, we make sure to use the same algorithmic initialization for SGD (e.g., we use the same initial model parameters), and the same simulation seed.

Parameters. Next, we focus on the parameters that govern the distributed system setup underlying our experiments. We configure the system architecture as follows: we consider a “parameter server” setup, whereby 8 worker machines are connected to a master by a simple network model: we do not simulate network congestion, we impose fair bandwidth sharing, and we do not account for message routing overheads.

In our system simulation, both computation and communication costs can be modeled according to a variety of distributions. To simplify our analysis, in this work we use uniformly distributed computation times with a small support, that are indicative of an homogeneous system. Instead of directly controlling the staleness of gradient updates, as done in other studies (Damaskinos et al., 2018; Dai et al., 2019), we indirectly induce staleness by imposing synthetic network delays, which we generate according to an exponential distribution with rate λ (the inverse of the mean).

Notice that the interplay between communication delay and staleness is subtle: we provide a comprehensive description of the staleness generation process in Appendix B, with illustrations that help understanding the shape of the τ_t distribution.

An intuitive view on the role of the exponential delay rate λ , which is the main system parameter that we vary in our simulations, is as follows. Small values of λ correspond to a system whereby a majority of gradient updates produced by worker machines have a small staleness; however, the tails of the delay distribution produce some outliers, which suffer from large staleness values (up to 40 algorithmic steps late). By increasing λ , we strengthen the impact of staleness: a large fraction of gradient updates is affected by moderately high staleness values, but the change in the delay distribution induces fewer outliers. When λ tends to infinity, the system we designed behaves as a round-robin scheme: each gradient updates is systematically late by a number of timesteps that is proportional to the number of workers in the system. In this paper, however, we gloss over this degenerate system configuration.

Models and datasets. We consider a classification task, where we train two CNN variants of increasing model complexity, to gain insight on the role of sparsification for large Deep network models. First, we study the behavior of LENET, using the MNIST dataset, then we move to RESNET-18, using the

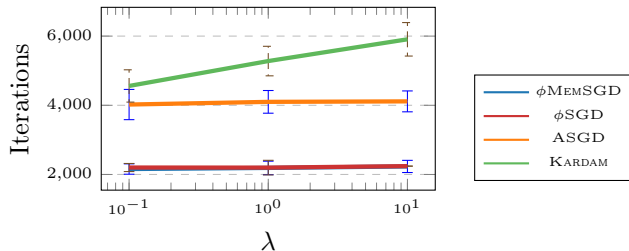


Figure 2: Comparison of convergence iterations to reach a target 95% accuracy, according to increasingly challenging staleness distributions, as imposed by the exponential delay rate λ . Results for LENET on MNIST. For sparsified methods, ϕ MEMSGD uses $\rho = 10\%$, while ϕ SGD uses $\rho = 50\%$.

CIFAR10 dataset. Overall, the model parameter and gradients dimensionality are approximately $d \in \{60K, 11M\}$ for LENET and RESNET-18, respectively. We use a training mini-batch size of 64 and a testing mini-batch size of 256 samples. Additional details are available in Appendix D.

3.2 Comparative analysis

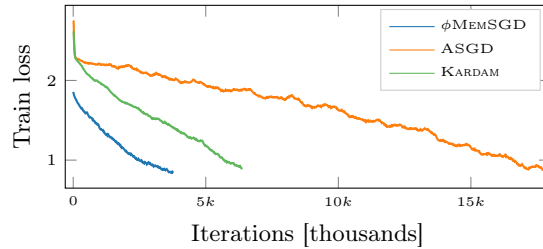
We compare ϕ SGD and ϕ MEMSGD with ASGD and KARDAM by measuring the number of model updates (that is, the number of iterations) required to achieve a target accuracy, which we set to 95% for LENET on MNIST and 70% for RESNET-18 on CIFAR10. We vary the exponential delay rate λ , and use the best sparsification coefficient ρ . We discuss how ρ can be tuned in Section 3.3.

Figure 2 illustrates results obtained using a LENET architecture with the MNIST dataset. It is evident that sparsified methods outperform alternatives, for all values of the exponential delay rate λ .

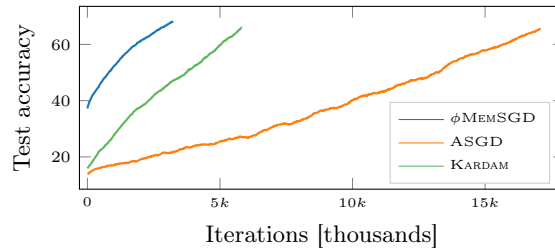
Overall, sparsification induces almost a 2x speedups w.r.t. ASGD, and much more when compared to KARDAM. Although ϕ MEMSGD and ϕ SGD seem to overlap, due to the scale of the plot, the memory based variant has, as expected, an edge on the memory-less method. It is also important to notice that ϕ MEMSGD uses a much lower sparsification rate than ϕ SGD:² this results clarifies the impact of memory-based error correction as a method to recover lost information due to aggressive sparsification. Additionally, our experiments indicate that the KARDAM algorithm suffers from an aggressive exponential dampening function: as soon as gradient staleness increases beyond few model iterates, their contribution is nullified, which implies a large number of iterations can go wasted before convergence.

Finally, note that we explicitly report “iterations” rather than wall-clock times, as we are not interested in measuring the well-known benefits of sparsification in

²For sparsified methods, we report results with the second best sparsification coefficient. Indeed, the impact on performance is negligible w.r.t. the potential savings of more sparse vectors. See also Section 3.3.



(a) RESNET-18 Training Loss



(b) RESNET-18 Test accuracy

Figure 3: Training loss and test accuracy as a function of algorithmic progress, for RESNET-18 on CIFAR10 to reach a target accuracy of 70%; exponential delay rate $\lambda = 1.0$, ϕ MEMSGD with $\rho = 1\%$.

terms of reduced communication costs.

Figure 3a and Figure 3b offer a detailed view of the training loss and test accuracy for the RESNET-18 architecture, to reach a target 70% accuracy. Here we set the exponential delay rate to $\lambda = 1.0$, which corresponds to a system in which a large fraction of model updates suffer from a moderate staleness. We compare the three SGD variants making sure they are equally initialized, we use the same seed, and tune their parameters individually.

Sparsification induces faster convergence times: ϕ MEMSGD consistently outperforms both ASGD and KARDAM. In particular, we notice that we chose the sparsification coefficient $\rho = 1\%$, which yields the best results in our experiments. By using only few principal components of gradient updates, ϕ MEMSGD requires far less iterations to reach the target accuracy.

3.3 Tuning gradient sparsification

Using theorem 2.1 alone, it can be difficult to understand how ρ can be tuned. Next, we focus on the LENET architecture using the MNIST, and set a target accuracy of 95%.

The results in Figure 4a show, for a given exponential delay rate $\lambda = 0.1$, the impact of different values of the sparsification coefficient ρ on algorithmic progress. We notice a stark difference between ϕ MEMSGD and ϕ SGD: the

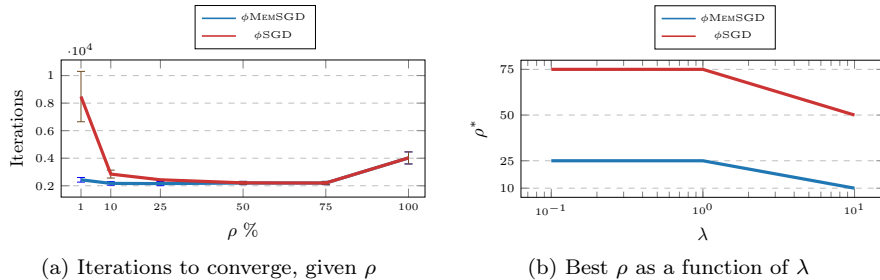


Figure 4: Detailed study to understand how to tune the sparsification ρ , for LENEt on MNIST. a) Number of iterations to reach 91% accuracy as a function of ρ , when $\lambda = 0.1$; b) Values of ρ that yield the best convergence rate as a function of the exponential delay rate λ .

latter is much more sensitive to appropriate choices of ρ , and requires larger coefficients. For ϕ MEMSGD, instead, aggressive sparsification doesn’t penalize performance too much: in the interest of saving bandwidth, a good practice is then to choose small values of ρ . In our experiments we used $\rho = 10\%$, but even smaller values do not incur in substantial performance penalty. If we increase ρ beyond 75%, thus studying the limit for which sparsified variants behave as ASGD, performance degrades. Beyond $\rho = 50\%$ both ϕ MEMSGD and ϕ SGD behave similarly, and overlap in the graphs we plot. An avenue for future empirical work is to understand how to tune ρ as a function of model dimensionality d .

Whereas in this work we are interested in convergence rates, other works study the “wall-clock” time to convergence. In this optics, even aggressive sparsification can be viable, as the cost per iteration (in terms of transmission times), decreases drastically. Also, note that the top- k operator can execute efficiently on a GPU (Shanbhag et al., 2018), so that computational costs per iterations are equivalent to standard SGD.

Figure 4b shows, for an increasing exponential delay rate λ , the best sparsification coefficient ρ to obtain the smallest number of iterations to reach a given target test accuracy. We notice that ϕ MEMSGD is less sensitive to the staleness distribution in the system, and settles for lower sparsification ρ than its memory-less counterpart. Interestingly, both approaches appear to achieve better performance by aggressive sparsification when the system conditions degrade and the impact of staleness on gradient updates is more severe. In such cases, maybe counter-intuitively, relying on only few, principal gradient components is more useful to help the optimization process to reach a local minimum, rather than using the additional information contained in stochastic gradient updates.

4 Conclusion

In this work we focused on the role of asynchrony in distributed stochastic optimization, and studied sparsification methods as ways to mitigate the effects of staleness affecting the asynchronous SGD algorithm. For the first time, we provided a concise analysis of asynchronous, sparsified SGD, and showed that it converges asymptotically as $\mathcal{O}\left(1/\sqrt{T}\right)$. Intuitively, top- k sparsification restricts the path taken by model iterates in the optimization landscape to follow the principal components of a stochastic gradient update.

We complemented our theoretical results with a thorough experimental campaign. Our results covered both variants of sparsified SGD, with and without memory, and alternative approaches from the literature, and demonstrated substantial benefits even with high sparsification levels.

Our future plan is to give a theoretical proof to why sparsification helps. Several studies show that the landscape of the loss surface of Deep models is typically sparse (Sagun et al., 2017; Draxler et al., 2018; Karakida et al., 2018). This further supports the intuition that working on sparsified gradients of the loss function should benefit convergence.

References

- N. Dryden , T. Moon , S. A. Jacobs , and B. V. Essen. Communication quantization for data-parallel training of deep neural networks. In *2016 2nd Workshop on Machine Learning in HPC Environments (MLHPC)*, pages 1–8, Nov 2016. doi: 10.1109/MLHPC.2016.004.
- A. F. Aji and K. Heafield. Sparse communication for distributed gradient descent. *arXiv*, abs/1704.05021, 2017. URL <http://arxiv.org/abs/1704.05021>.
- D. Alistarh, D. Grubic, J. Li, R. Tomioka, and M. Vojnovic. QSGD : Communication-efficient SGD via gradient quantization and encoding. In *Advances in Neural Information Processing Systems 30*, pages 1709–1720. Curran Associates, Inc., 2017. URL <http://papers.nips.cc/paper/6768-qsgd-communication-efficient-sgd-via-gradient-quantization-and-encoding.pdf>.
- D. Alistarh, T. Hoefler, M. Johansson, N. Konstantinov, S. Khirirat, and C. Renggli. The convergence of sparsified gradient methods. In S. Bengio, H. Wallach, H. Larochelle, K. Grauman, N. Cesa-Bianchi, and R. Garnett, editors, *Advances in Neural Information Processing Systems*, pages 5973–5983. Curran Associates, Inc., 2018. URL <http://papers.nips.cc/paper/7837-the-convergence-of-sparsified-gradient-methods.pdf>.
- J. Bernstein, Y.-X. Wang, K. Azizzadenesheli, and A. Anandkumar. Compression by the signs: distributed learning is a two-way street. In *ICLR*, 2018a.

- J. Bernstein, Y.-X. Wang, K. Azizzadenesheli, and A. Anandkumar. signsgd: Compressed optimisation for non-convex problems. *Proceedings of Machine Learning Research*, 80:560–569, 2018b.
- L. Bottou. Large-scale machine learning with stochastic gradient descent. In *Proceedings of COMPSTAT’2010*, pages 177–186. Springer, 2010.
- L. Bottou, F. E. Curtis, and J. Nocedal. Optimization methods for large-scale machine learning. *SIAM Review*, 60(2):223–311, 2018. doi: 10.1137/16M1080173. URL <https://doi.org/10.1137/16M1080173>.
- J. Chen, R. Monga, S. Bengio, and R. Jozefowicz. Revisiting distributed synchronous sgd. In *International Conference on Learning Representations Workshop Track*, 2016. URL <https://arxiv.org/abs/1604.00981>.
- T. Chilimbi, Y. Suzue, J. Apacible, and K. Kalyanaraman. Project adam: Building an efficient and scalable deep learning training system. In *11th USENIX Symposium on Operating Systems Design and Implementation (OSDI 14)*, pages 571–582, Broomfield, CO, 2014. USENIX Association. ISBN 978-1-931971-16-4. URL <https://www.usenix.org/conference/osdi14/technical-sessions/presentation/chilimbi>.
- W. Dai, Y. Zhou, N. Dong, H. Zhang, and E. P. Xing. Toward understanding the impact of staleness in distributed machine learning. In *Proceedings of the 7th International Conference on Learning Representations, ICLR’19*, 2019.
- G. Damaskinos, E. M. El Mhamdi, R. Guerraoui, R. Patra, and M. Taziki. Asynchronous byzantine machine learning (the case of sgd). In J. Dy and A. Krause, editors, *Proceedings of the 35th International Conference on Machine Learning*, volume 80 of *Proceedings of Machine Learning Research*, pages 1145–1154, Stockholm, Sweden, 10–15 Jul 2018. PMLR. URL <http://proceedings.mlr.press/v80/damaskinos18a.html>.
- C. M. De Sa, C. Zhang, K. Olukotun, and C. Re. Taming the wild: A unified analysis of hogwild-style algorithms. In *Advances in neural information processing systems*, pages 2674–2682, 2015.
- J. Dean, G. Corrado, R. Monga, K. Chen, M. Devin, M. Mao, M. aurelio Ranzato, A. Senior, P. Tucker, K. Yang, Q. V. Le, and A. Y. Ng. Large scale distributed deep networks. In F. Pereira, C. J. C. Burges, L. Bottou, and K. Q. Weinberger, editors, *Advances in Neural Information Processing Systems 25*, pages 1223–1231. Curran Associates, Inc., 2012. URL <http://papers.nips.cc/paper/4687-large-scale-distributed-deep-networks.pdf>.
- F. Draxler, K. Veschgini, M. Salmhofer, and F. A. Hamprecht. Essentially no barriers in neural network energy landscape. *arXiv preprint arXiv:1803.00885*, 2018.

- S. Dutta, G. Joshi, S. Ghosh, P. Dube, and P. Nagpurkar. Slow and stale gradients can win the race: Error-runtime trade-offs in distributed SGD . In A. Storkey and F. Perez-Cruz, editors, *Proceedings of the Twenty-First International Conference on Artificial Intelligence and Statistics*, pages 803–812. PMLR, 2018. URL <http://proceedings.mlr.press/v84/dutta18a.html>.
- S. Ghadimi and G. Lan. Stochastic first-and zeroth-order methods for nonconvex stochastic programming. *SIAM Journal on Optimization*, 23(4):2341–2368, 2013.
- P. Goyal, P. Dollar, R. B. Girshick, P. Noordhuis, L. Wesolowski, A. Kyrola, A. Tulloch, Y. Jia, and K. He. Accurate, large minibatch sgd: Training image net in 1 hour. *arXiv*, abs/1706.02677, 2017.
- Q. Ho, J. Cipar, H. Cui, S. Lee, J. K. Kim, P. B. Gibbons, G. A. Gibson, G. Ganger, and E. P. Xing. More effective distributed ML via a stale synchronous parallel parameter server. In C. J. C. Burges, L. Bottou, M. Welling, Z. Ghahramani, and K. Q. Weinberger, editors, *Advances in Neural Information Processing Systems 26*, pages 1223–1231. Curran Associates, Inc., 2013. URL <http://papers.nips.cc/paper/4894-more-effective-distributed-ml-via-a-stale-synchronous-parallel-parameter-server.pdf>.
- J. Jiang, B. Cui, C. Zhang, and L. Yu. Heterogeneity-aware distributed parameter servers. In *Proceedings of the 2017 ACM International Conference on Management of Data*, SIGMOD ’17, pages 463–478, New York, NY, USA, 2017. ACM. ISBN 978-1-4503-4197-4. doi: 10.1145/3035918.3035933. URL <http://doi.acm.org/10.1145/3035918.3035933>.
- R. Karakida, S. Akaho, and S.-i. Amari. Universal statistics of fisher information in deep neural networks: mean field approach. *arXiv preprint arXiv:1806.01316*, 2018.
- M. Li, D. G. Andersen, J. W. Park, A. J. Smola, A. Ahmed, V. Josifovski, J. Long, E. J. Shekita, and B.-Y. Su. Scaling distributed machine learning with the parameter server. In *11th USENIX Symposium on Operating Systems Design and Implementation (OSDI 14)*, pages 583–598, Broomfield, CO, 2014. USENIX Association. ISBN 978-1-931971-16-4. URL https://www.usenix.org/conference/osdi14/technical-sessions/presentation/li_mu.
- X. Lian, Y. Huang, Y. Li, and J. Liu. Asynchronous parallel stochastic gradient for nonconvex optimization. In *Advances in Neural Information Processing Systems*, pages 2737–2745, 2015.
- T. Lin, S. U. Stich, and M. Jaggi. Don’t use large mini-batches, use local SGD . *arXiv*, abs/1808.07217, 2018.
- J. Liu and S. J. Wright. Asynchronous stochastic coordinate descent: Parallelism and convergence properties. *SIAM Journal on Optimization*, 25(1):351–376, 2015.

- S. Mandt, M. D. Hoffman, and D. M. Blei. Stochastic gradient descent as approximate bayesian inference. *The Journal of Machine Learning Research*, 18(1):4873–4907, 2017.
- I. Mitliagkas, C. Zhang, S. Hadjis, and C. Re. Asynchrony begets momentum, with an application to deep learning. In *2016 54th Annual Allerton Conference on Communication, Control, and Computing (Allerton)*, pages 997–1004. IEEE, 2016.
- E. Moulines and F. R. Bach. Non-asymptotic analysis of stochastic approximation algorithms for machine learning. In J. Shawe-Taylor, R. S. Zemel, P. L. Bartlett, F. Pereira, and K. Q. Weinberger, editors, *Advances in Neural Information Processing Systems 24*, pages 451–459. Curran Associates, Inc., 2011. URL <http://papers.nips.cc/paper/4316-non-asymptotic-analysis-of-stochastic-approximation-algorithms-for-machine-learning.pdf>.
- B. Recht, C. Re, S. Wright, and F. Niu. Hogwild: A lock-free approach to parallelizing stochastic gradient descent. In J. Shawe-Taylor, R. S. Zemel, P. L. Bartlett, F. Pereira, and K. Q. Weinberger, editors, *Advances in Neural Information Processing Systems*, pages 693–701. Curran Associates, Inc., 2011. URL <http://papers.nips.cc/paper/4390-hogwild-a-lock-free-approach-to-parallelizing-stochastic-gradient-descent.pdf>.
- H. Robbins and S. Monro. A stochastic approximation method. *Annals of Mathematical Statistics*, 22:400–407, 1951.
- L. Sagun, U. Evci, V. U. Guney, Y. Dauphin, and L. Bottou. Empirical analysis of the hessian of over-parametrized neural networks. *arXiv preprint arXiv:1706.04454*, 2017.
- A. M. Saxe, Y. Bansal, J. Dapello, M. Advani, A. Kolchinsky, B. D. Tracey, and D. D. Cox. On the information bottleneck theory of deep learning. In *Proceedings of the 6th International Conference on Learning Representations, ICLR’18*, 2018.
- F. Seide, H. Fu, J. Droppo, G. Li, and D. Yu. 1-bit stochastic gradient descent and its application to data-parallel distributed training of speech DNN s. In *Fifteenth Annual Conference of the International Speech Communication Association*, 2014.
- A. Shanbhag, H. Pirk, and S. Madden. Efficient top-k query processing on massively parallel hardware. In *Proceedings of the 2018 International Conference on Management of Data*, pages 1557–1570. ACM, 2018.
- R. Shwartz-Ziv and N. Tishby. Opening the black box of deep neural networks via information. *arXiv preprint arXiv:1703.00810*, 2017.
- S. U. Stich. Local SGD converges fast and communicates little. In *Proceedings of the 7th International Conference on Learning Representations, ICLR’19*, 2019.

- S. U. Stich, J.-B. Cordonnier, and M. Jaggi. Sparsified SGD with memory. In S. Bengio, H. Wallach, H. Larochelle, K. Grauman, N. Cesa-Bianchi, and R. Garnett, editors, *Advances in Neural Information Processing Systems 31*, pages 4447–4458. Curran Associates, Inc., 2018. URL <http://papers.nips.cc/paper/7697-sparsified-sgd-with-memory.pdf>.
- N. Strom. Scalable distributed DNN training using commodity GPU cloud computing. In *Sixteenth Annual Conference of the International Speech Communication Association*, 2015.
- J. Wangni, J. Wang, J. Liu, and T. Zhang. Gradient sparsification for communication-efficient distributed optimization. In S. Bengio, H. Wallach, H. Larochelle, K. Grauman, N. Cesa-Bianchi, and R. Garnett, editors, *Advances in Neural Information Processing Systems*, pages 1299–1309. Curran Associates, Inc., 2018. URL <http://papers.nips.cc/paper/7405-gradient-sparsification-for-communication-efficient-distributed-optimization.pdf>.
- W. Wen, C. Xu, F. Yan, C. Wu, Y. Wang, Y. Chen, and H. Li. Terngrad: Ternary gradients to reduce communication in distributed deep learning. In I. Guyon, U. V. Luxburg, S. Bengio, H. Wallach, R. Fergus, S. Vishwanathan, and R. Garnett, editors, *Advances in Neural Information Processing Systems 30*, pages 1509–1519. Curran Associates, Inc., 2017. URL <http://papers.nips.cc/paper/6749-terngrad-ternary-gradients-to-reduce-communication-in-distributed-deep-learning.pdf>.
- Y. You, I. Gitman, and B. Ginsburg. Scaling sgd batch size to 32k for image net training. *arXiv, abs/1708.03888*, 6, 2017.
- H. Yu, S. Yang, and S. Zhu. Parallel restarted SGD with faster convergence and less communication: Demystifying why model averaging works for deep learning. In *AAAI 2019*, 2019.
- J. Zhang, C. D. Sa, I. Mitliagkas, and C. Re. Parallel sgd: When does averaging help? *arXiv, abs/1606.07365*, 2016.

A Proof of Theorem

In this subsection we build all the useful tools to formalize the proof of 2.1. In A.1 we prove the k -contraction lemma, in A.2 we restate assumptions for simplicity, we derive useful facts in A.3, derive a tighter bounding term for the sum of magnitudes of stale gradients in A.4, and finally derive the full proof of the convergence theorem in A.5.

A.1 Proof of 2.1

Given a vector $\mathbf{u} \in \mathbb{R}^d$, a parameter $1 \leq k \leq d$, and the top- k operator $\Phi_k(\mathbf{u}) : \mathbb{R}^d \rightarrow \mathbb{R}^d$ defined in 2.1, we have that:

$$\|\Phi_k(\mathbf{u})\|^2 \geq \frac{k}{d}\|\mathbf{u}\|^2$$

In fact we can write $\|\mathbf{u}\|^2$ as follows:

$$\begin{aligned} \|\Phi_k(\mathbf{u})\|^2 &= \|\mathbf{u}\|^2 - \|\mathbf{u} - \Phi_k(\mathbf{u})\|^2 \\ &\geq \|\mathbf{u}\|^2 - \left(1 - \frac{k}{d}\right)\|\mathbf{u}\|^2 = \frac{k}{d}\|\mathbf{u}\|^2 \end{aligned} \quad (2)$$

Where the inequality is obtained by simply applying the k-contraction property.

A.2 Recap of Assumptions

We start by rewriting for simplicity assumptions 1 to 5:

1. $f(\mathbf{x})$ is continuously differentiable and bounded below: $\inf_x f(\mathbf{x}) > -\infty$
2. $\nabla f(\mathbf{x})$ is L -Lipschitz smooth:

$$\forall \mathbf{x}, \mathbf{y} \in \mathbb{R}^d, \|\nabla f(\mathbf{x}) - \nabla f(\mathbf{y})\| \leq L\|\mathbf{x} - \mathbf{y}\|$$

3. The variance of the (mini-batch) stochastic gradients is bounded:

$$\mathbb{E} \left[\|\mathbf{g}(\mathbf{x}_t, \xi_t) - \nabla f(\mathbf{x}_t)\|^2 \right] \leq \sigma^2,$$

where $\sigma^2 > 0$ is a constant.

4. The staleness is bounded, that is: $t - S \leq \tau_t \leq t$, $S \geq 0$. In other words, the model staleness τ_t satisfies the inequality $t - \tau_t \leq S$. We call $S \geq 0$ the maximum delay.
5. The cosine distance between sparse, stale and stochastic gradient and the full one is lower bounded

$$\frac{\mathbb{E} [\langle \Phi_k(\mathbf{g}(\mathbf{x}_{\tau_t}, \xi_t)), \nabla f(\mathbf{x}_t) \rangle]}{\mathbb{E} [\|\Phi_k(\mathbf{g}(\mathbf{x}_{\tau_t}, \xi_t))\| \|\nabla f(\mathbf{x}_t)\|]} = \mu_t \geq \mu$$

Notice moreover that ξ_t is statistically independent from $\{\mathbf{x}_0, \dots, \mathbf{x}_t\}$.

A.3 Useful facts

Starting from 2 we can write that:

$$f(\mathbf{x}) \leq f(\mathbf{y}) + \langle \mathbf{x} - \mathbf{y}, \nabla f(\mathbf{y}) \rangle + \frac{L}{2}\|\mathbf{x} - \mathbf{y}\|^2 \quad \forall \mathbf{x}, \mathbf{y}$$

Trivially we can rewrite this inequality by using as arguments the two vectors $\mathbf{x}_t, \mathbf{x}_{t+1}$:

$$\begin{aligned}
f(\mathbf{x}_{t+1}) &\leq f(\mathbf{x}_t) + \langle \mathbf{x}_{t+1} - \mathbf{x}_t, \nabla f(\mathbf{x}_t) \rangle + \\
&\quad + \frac{L}{2} \|\mathbf{x}_{t+1} - \mathbf{x}_t\|^2 \\
&= f(\mathbf{x}_t) - \eta_t \langle \Phi_k[\mathbf{g}(\mathbf{x}_{\tau_t}, \xi_t)], \nabla f(\mathbf{x}_t) \rangle \\
&\quad + \frac{\eta_t^2 L}{2} \|\Phi_k[\mathbf{g}(\mathbf{x}_{\tau_t}, \xi_t)]\|^2
\end{aligned} \tag{3}$$

where the last equality is due to $\mathbf{x}_{t+1} = \mathbf{x}_t - \eta_t \Phi_k(\mathbf{g}(\mathbf{x}_{\tau_t}, \xi_t))$. Notice that even if \mathbf{x}_t as well as ξ_t, τ_t and consequently $f(\mathbf{x}_t)$ and $g(\mathbf{x}_t)$ are random processes, due to the geometric constraints imposed on the cost function, the above inequality holds with probability 1.

The second useful quantity we derive is a bound for squared magnitude of $\mathbf{g}(\mathbf{x}_t, \xi_t)$. We start with 3.

Before proceeding, we introduce the following notation: Ω is the set of ALL random variables (i.e. $\Omega = \{\xi_0, \dots, \xi_t, \mathbf{x}_0, \dots, \mathbf{x}_t, \tau_0, \dots, \tau_t\}$), furthermore, we indicate with $\sim \xi_t$ the set difference between Ω and ξ_t .

We write:

$$\begin{aligned}
&\mathbb{E}_\Omega \left[\|\mathbf{g}(\mathbf{x}_t, \xi_t) - \nabla f(\mathbf{x}_t)\|^2 \right] \\
&= \mathbb{E}_\Omega \left[\|\mathbf{g}(\mathbf{x}_t, \xi_t) - \mathbb{E}_{\xi_t}(\mathbf{g}(\mathbf{x}_t, \xi_t))\|^2 \right] \\
&= \mathbb{E}_{\sim \xi_t} \left[\mathbb{E}_{\xi_t} \left[\|\mathbf{g}(\mathbf{x}_t, \xi_t) - \mathbb{E}_{\xi_t}(\mathbf{g}(\mathbf{x}_t, \xi_t))\|^2 \right] \right] \\
&= \mathbb{E}_{\sim \xi_t} \left[\mathbb{E}_{\xi_t} [\|\mathbf{g}(\mathbf{x}_t, \xi_t)\|^2] - \|\mathbb{E}_{\xi_t}(\mathbf{g}(\mathbf{x}_t, \xi_t))\|^2 \right] \\
&= \mathbb{E}_\Omega [\|\mathbf{g}(\mathbf{x}_t, \xi_t)\|^2] - \mathbb{E}_\Omega [\|\nabla f(\mathbf{x}_t)\|^2] \leq \sigma^2
\end{aligned}$$

from which:

$$\mathbb{E}_\Omega [\|\mathbf{g}(\mathbf{x}_t, \xi_t)\|^2] \leq \mathbb{E}_\Omega [\|\nabla f(\mathbf{x}_t)\|^2] + \sigma^2 \tag{4}$$

A.4 Bounding magnitudes of delayed gradients

Differently from Dai et al. (2019), we derive a tighter bound for the following term:

$$\sum_{t=0}^{T-1} \eta_t^2 \mathbb{E} \left[\|\nabla f(\mathbf{x}_{\tau_t})\|^2 \right] \tag{5}$$

Indeed, thanks to the fact that η_t is a decreasing sequence, and using the law of total expectation:

$$\begin{aligned}
& \sum_{t=0}^{T-1} \eta_t^2 \mathbb{E} \left[\|\nabla f(\mathbf{x}_{\tau_t})\|^2 \right] \\
&= \sum_{t=0}^{T-1} \eta_t^2 \sum_{l=t-S}^t \Pr(\tau_t = l) \mathbb{E} \left[\|\nabla f(\mathbf{x}_l)\|^2 \right] \\
&\leq \sum_{t=0}^{T-1} \sum_{l=t-S}^t \eta_l^2 \Pr(\tau_t = l) \mathbb{E} \left[\|\nabla f(\mathbf{x}_l)\|^2 \right]
\end{aligned}$$

Before proceeding, it is useful to introduce a new random quantity, the delay D , distributed according to some probability density function $\Pr(D = i) = \pi_i$. Notice that the true relationship between $\Pr(\tau_t)$ and $\Pr(D)$ is:

$$\Pr(\tau_t = l) = \frac{\pi_{t-l}}{\sum_{i=0}^{\min(t,S)} \pi_i}.$$

Since $t - S \leq \tau_t \leq t$, obviously the delay variable D has support boundend in $[0, S]$. Moreover, to reduce clutter, we define: $\psi_l = \eta_l^2 \mathbb{E} \left[\|\nabla f(\mathbf{x}_l)\|^2 \right]$.

Now, we can continue our derivation as:

$$\begin{aligned}
& \sum_{t=0}^{T-1} \sum_{l=t-S}^t \frac{\pi_{t-l}}{\sum_{i=0}^{\min(t,S)} \pi_i} \psi_l = \\
& \frac{\pi_S \psi_{-S+0} + \pi_{S-1} \psi_{-S+1} + \cdots + \pi_1 \psi_{-1} + \pi_0 \psi_0}{\pi_0} + \\
& \frac{\pi_S \psi_{-S+1} + \pi_{S-1} \psi_{-S+2} + \cdots + \pi_1 \psi_0 + \pi_0 \psi_1}{\pi_0 + \pi_1} + \\
& \frac{\pi_S \psi_{-S+2} + \pi_{S-1} \psi_{-S+3} + \cdots + \pi_1 \psi_1 + \pi_0 \psi_2}{\pi_0 + \pi_1 + \pi_2} + \\
& \frac{\pi_S \psi_{-S+3} + \pi_{S-1} \psi_{-S+4} + \cdots + \pi_1 \psi_2 + \pi_0 \psi_3}{\pi_0 + \pi_1 + \pi_2 + \pi_3} + \\
& \cdots \\
& \frac{\pi_S \psi_{T-S} + \cdots + \pi_1 \psi_{T-1} + \pi_0 \psi_T}{1} \leq
\end{aligned}$$

$$\begin{aligned}
& \pi_S \psi_{-S+0} + \pi_{S-1} \psi_{-S+1} + \cdots + \pi_1 \psi_{-1} + \pi_0 \psi_0 + C_0 + \\
& \pi_S \psi_{-S+1} + \pi_{S-1} \psi_{-S+2} + \cdots + \pi_1 \psi_0 + \pi_0 \psi_1 + C_1 + \\
& \pi_S \psi_{-S+2} + \pi_{S-1} \psi_{-S+3} + \cdots + \pi_1 \psi_1 + \pi_0 \psi_2 + C_2 + \\
& \pi_S \psi_{-S+3} + \pi_{S-1} \psi_{-S+4} + \cdots + \pi_1 \psi_2 + \pi_0 \psi_3 + C_3 + \\
& \cdots \\
& \pi_S \psi_{T-S} + \cdots + \pi_1 \psi_{T-1} + \pi_0 \psi_T + 0 \\
& \leq \sum_{t=0}^{T-1} \psi_t + C \\
& = \sum_{t=0}^{T-1} \eta_t^2 \mathbb{E} \left[\|\nabla f(\mathbf{x}_t)\|^2 \right] + C
\end{aligned}$$

where C is a suitable, finite, constant. We thus proved a strict bound on the sum of magnitudes of delayed gradients as

$$\sum_{t=0}^{T-1} \eta_t^2 \mathbb{E} \left[\|\nabla f(\mathbf{x}_{\tau_t})\|^2 \right] \leq \sum_{t=0}^{T-1} \eta_t^2 \mathbb{E} \left[\|\nabla f(\mathbf{x}_t)\|^2 \right] + C.$$

A.5 Derivation of the theorem

We start the derivation from 3. We rearrange the inequality to bound the increment of cost function at time instant t as:

$$\begin{aligned}
f(\mathbf{x}_{t+1}) - f(\mathbf{x}_t) & \leq -\eta_t \langle \Phi_k[\mathbf{g}(\mathbf{x}_{\tau_t}, \xi_t)], \nabla f(\mathbf{x}_t) \rangle \\
& \quad + \frac{\eta_t^2 L}{2} \|\Phi_k[\mathbf{g}(\mathbf{x}_{\tau_t}, \xi_t)]\|^2
\end{aligned}$$

Written in this form, we are still dealing with random quantities. We are interested in taking the expectation of above inequality with respect to **all** random processes. Then:

$$\begin{aligned}
& \mathbb{E}_\Omega [f(\mathbf{x}_{t+1}) - f(\mathbf{x}_t)] \\
& \leq \mathbb{E}_\Omega [-\eta_t \langle \Phi_k[\mathbf{g}(\mathbf{x}_{\tau_t}, \xi_t)], \nabla f(\mathbf{x}_t) \rangle \\
& \quad + \frac{\eta_t^2 L}{2} \|\Phi_k[\mathbf{g}(\mathbf{x}_{\tau_t}, \xi_t)]\|^2]
\end{aligned}$$

The strategy to continue the proof is to find an upper bound for the expectation term $\mathbb{E}_\Omega \left[\|\Phi_k[\mathbf{g}(\mathbf{x}_{\tau_t}, \xi_t)]\|^2 \right]$ and a lower bound for the expectation term $\mathbb{E}_\Omega [\langle \Phi_k[\mathbf{g}(\mathbf{x}_{\tau_t}, \xi_t)], \nabla f(\mathbf{x}_t) \rangle]$. We start with the upper bound as:

$$\begin{aligned}
& \mathbb{E}_\Omega \left[\|\Phi_k[\mathbf{g}(\mathbf{x}_{\tau_t}, \xi_t)]\|^2 \right] \leq \mathbb{E}_\Omega \left[\|\mathbf{g}(\mathbf{x}_{\tau_t}, \xi_t)\|^2 \right] \\
& \leq \mathbb{E} \left[\|\nabla f(\mathbf{x}_{\tau_t})\|^2 \right] + \sigma^2,
\end{aligned}$$

where the first inequality is a trivial consequence of sparsification and the second is the application of 4.

As anticipated, we aim at lower bounding the term: $\mathbb{E}_\Omega [\langle \Phi_k [\mathbf{g}(\mathbf{x}_{\tau_t}, \xi_t)], \nabla f(\mathbf{x}_t) \rangle]$. We start with 5 and write:

$$\begin{aligned} & \mathbb{E}_\Omega [\langle \Phi_k(\mathbf{g}(\mathbf{x}_{\tau_t}, \xi_t)), \nabla f(\mathbf{x}_t) \rangle] \\ & \geq \mu \mathbb{E}_\Omega [\|\Phi_k(\mathbf{g}(\mathbf{x}_{\tau_t}, \xi_t))\| \|\nabla f(\mathbf{x}_t)\|] \\ & = \mu \mathbb{E}_{\sim \xi_t} [\mathbb{E}_{\xi_t} [\|\Phi_k(\mathbf{g}(\mathbf{x}_{\tau_t}, \xi_t))\| \|\nabla f(\mathbf{x}_t)\|]] \\ & = \mu \mathbb{E}_{\sim \xi_t} [\mathbb{E}_{\xi_t} [\|\Phi_k(\mathbf{g}(\mathbf{x}_{\tau_t}, \xi_t))\|] \|\nabla f(\mathbf{x}_t)\|] \end{aligned}$$

We focus on the term $\mathbb{E}_{\xi_t} [\|\Phi_k(\mathbf{g}(\mathbf{x}_{\tau_t}, \xi_t))\|]$ and, thanks to the k -contraction property and the inequality of the norm of expected values, we can write:

$$\begin{aligned} & \mathbb{E}_\Omega [\langle \Phi_k(\mathbf{g}(\mathbf{x}_{\tau_t}, \xi_t)), \nabla f(\mathbf{x}_t) \rangle] \\ & \geq \mu \rho \mathbb{E}_{\sim \xi_t} [\mathbb{E}_{\xi_t} [\|\mathbf{g}(\mathbf{x}_{\tau_t}, \xi_t)\|] \|\nabla f(\mathbf{x}_t)\|] \\ & \geq \mu \rho \mathbb{E}_{\sim \xi_t} [\|\mathbb{E}_{\xi_t} [\mathbf{g}(\mathbf{x}_{\tau_t}, \xi_t)]\| \|\nabla f(\mathbf{x}_t)\|] \\ & = \mu \rho \mathbb{E}_{\sim \xi_t} [\|\nabla f(\mathbf{x}_{\tau_t})\| \|\nabla f(\mathbf{x}_t)\|] \end{aligned}$$

Before proceeding, we reasonably assume that:

$$\mathbb{E}_{\sim \xi_t} [\|\nabla f(\mathbf{x}_{\tau_t})\| \|\nabla f(\mathbf{x}_t)\|] \geq \mathbb{E}_{\sim \xi_t} [\|\nabla f(\mathbf{x}_t)\|^2], \quad (6)$$

since stale versions of the gradient should be larger, in magnitude, than recent versions.

Combining everything together we rewrite our initial inequality as:

$$\begin{aligned} \Delta_t & = \mathbb{E}_\Omega [f(\mathbf{x}_{t+1}) - f(\mathbf{x}_t)] \leq -\eta_t \rho \mu \mathbb{E}_{\sim \xi_t} [\|\nabla f(\mathbf{x}_t)\|^2] \\ & \quad + \frac{\eta_t^2 L}{2} \left(\mathbb{E}_{\sim \xi_t} [\|\nabla f(\mathbf{x}_{\tau_t})\|^2] + \sigma^2 \right). \end{aligned}$$

To derive a convergence bound it is necessary to sum all the increments over t from 0 to T :

$$\begin{aligned} \sum_{t=0}^{T-1} \Delta_t & \leq \sum_{t=0}^{T-1} \left(-\eta_t \rho \mu \mathbb{E}_{\sim \xi_t} [\|\nabla f(\mathbf{x}_t)\|^2] + \frac{\eta_t^2 L}{2} \left(\mathbb{E}_{\sim \xi_t} [\|\nabla f(\mathbf{x}_{\tau_t})\|^2] + \sigma^2 \right) \right) \\ & \leq \left(\sum_{t=0}^{T-1} -\eta_t \rho \mu \mathbb{E}_{\sim \xi_t} [\|\nabla f(\mathbf{x}_t)\|^2] + \frac{\eta_t^2 L}{2} \left(\mathbb{E}_{\sim \xi_t} [\|\nabla f(\mathbf{x}_t)\|^2] + \sigma^2 \right) \right) + C = \\ & \left(\sum_{t=0}^{T-1} \left(-\eta_t \rho \mu + \frac{\eta_t^2 L}{2} \right) \mathbb{E}_{\sim \xi_t} [\|\nabla f(\mathbf{x}_t)\|^2] + \frac{\eta_t^2 L}{2} \sigma^2 \right) + C, \end{aligned}$$

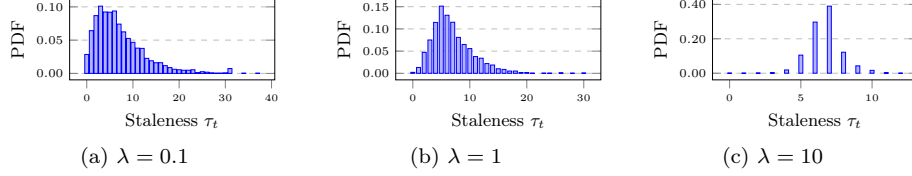


Figure 5: Staleness distribution for various rates λ of exponentially distributed t_{COMM} .

where for the second inequality we used the result of A.4.

We further manipulate the result by noticing that: $\sum_{t=0}^{T-1} \Delta_t = \mathbb{E}_{\Omega} [f(\mathbf{x}_{t+1}) - f(\mathbf{x}_0)]$. Moreover since $\Lambda = \mathbb{E}_{\Omega} [f(\mathbf{x}_0)] - \inf_{\mathbf{x}} f(\mathbf{x})$, it is easy to show that $\Lambda \geq \mathbb{E}_{\Omega} [f(\mathbf{x}_0) - f(\mathbf{x}_{t+1})] = -\sum_{t=0}^{T-1} \Delta_t$. We combine the bounds together as:

$$-\Lambda \leq \sum_{t=0}^{T-1} \Delta_t \leq \left(\sum_{t=0}^{T-1} \left(-\eta_t \rho \mu + \frac{\eta_t^2 L}{2} \right) \mathbb{E}_{\xi_t} [\|\nabla f(\mathbf{x}_t)\|^2] + \frac{\eta_t^2 L}{2} \sigma^2 \right) + C.$$

Then:

$$-\Lambda - C \leq \left(\sum_{t=0}^{T-1} \left(-\eta_t \rho \mu + \frac{\eta_t^2 L}{2} \right) \mathbb{E}_{\xi_t} [\|\nabla f(\mathbf{x}_t)\|^2] + \frac{\eta_t^2 L}{2} \sigma^2 \right),$$

and finally:

$$\left(\sum_{t=0}^{T-1} \left(\eta_t \rho \mu - \frac{\eta_t^2 L}{2} \right) \mathbb{E} [\|\nabla f(\mathbf{x}_t)\|^2] \right) \leq \left(\sum_{t=0}^{T-1} \left(\frac{\eta_t^2 L}{2} \sigma^2 \right) \right) + \Lambda + C.$$

We conclude that:

$$\min_{0 \leq t \leq T} \mathbb{E} [\|\nabla f(\mathbf{x}_t)\|^2] \leq \frac{\left(\sum_{t=0}^{T-1} \left(\frac{\eta_t^2 L}{2} \sigma^2 \right) \right) + \Lambda + C}{\sum_{t=0}^{T-1} \left(\eta_t \rho \mu - \frac{\eta_t^2 L}{2} \right)}.$$

We then proceed by proving the simple corollary 2.1 of Theorem 2.1. By choosing a suitable constant learning rate $\eta_t = \eta = \frac{\rho \mu}{L \sqrt{T}}$ we can rewrite the inequality as

$$\min_{0 \leq t \leq T} \mathbb{E} [\|\nabla f(\mathbf{x}_t)\|^2] \leq \frac{\left(T \left(\frac{\eta^2 L}{2} \sigma^2 \right) \right) + \Lambda'}{T \left(\eta \rho \mu - \frac{\eta^2 L}{2} \right)}.$$

where for simplicity we have defined $\Lambda' = \Lambda + C$.

We then notice that $\eta\rho\mu = \frac{(\rho\mu)^2}{L\sqrt{T}}$ and that $\frac{\eta^2L}{2} = \frac{(\rho\mu)^2}{2LT}$, consequently we can rewrite the upper bound as

$$\frac{\frac{(\rho\mu)^2\sigma^2}{2L} + \Lambda'}{\frac{(\rho\mu)^2\sqrt{T}}{L} - \frac{(\rho\mu)^2}{2L}} = \frac{\frac{(\rho\mu)^2\sigma^2}{2L} + \Lambda'}{\frac{(\rho\mu)^2}{L} \left(\sqrt{T} - \frac{1}{2}\right)}.$$

Since we are interested in \mathcal{O} convergence rate, we can safely assume that $\left(\sqrt{T} - \frac{1}{2}\right) \simeq \sqrt{T}$ and that thus

$$\begin{aligned} \min_{0 \leq t \leq T} \mathbb{E} \left[\|\nabla f(\mathbf{x}_t)\|^2 \right] &\lesssim \frac{\frac{(\rho\mu)^2\sigma^2}{2L} + \Lambda'}{\frac{(\rho\mu)^2}{L} \sqrt{T}} \\ &= \left(\frac{\sigma^2}{2} + \frac{\Lambda' L}{(\rho\mu)^2} \right) \frac{1}{\sqrt{T}} \end{aligned}$$

B A note on staleness

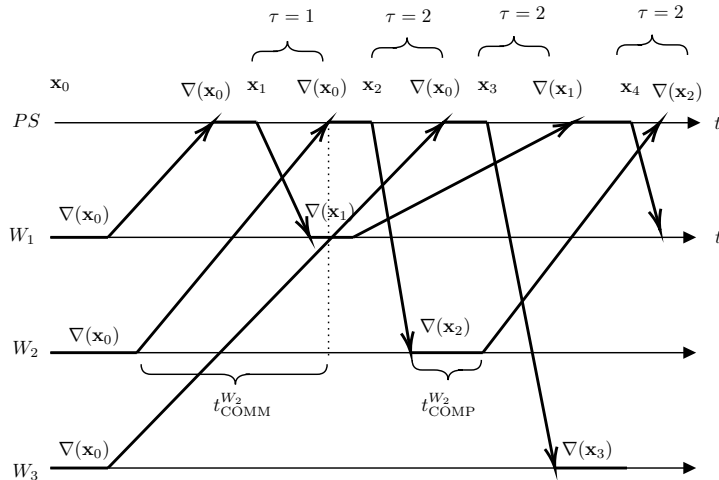
In this subsection we provide additional details to clarify the definition of staleness and its generating process in our empirical validation. We use 6 to illustrate these concepts, with a simple example. 6 is an abstract representation of the distributed architecture we consider in this work. It consists of a time-line for each machine in the system: one for the *parameter server* (PS), and one for each worker W_i ($i = 3$ in the Figure).

In our system model, the PS accepts contributions from workers and updates the current model iterate according to the variant of the SGD algorithm it implements. For example, in our experiments on ϕ SGD, it uses the algorithm outlined in 2.3. Then, the PS sends the new model to the worker machine that triggered the update. In 6, for example, W_1 sends its first gradient contribution using model \mathbf{x}_0 . The PS updates the current model iterate to \mathbf{x}_1 , and send it back to W_1 .

Workers, on the other hand, are tasked with the computation of the stochastic gradient of the loss function, that uses the latest model received from the PS. For example, in our experiments on ϕ SGD, workers compute the stochastic gradient using a mini-batch of training samples, then apply the sparsification operator Φ_k , and send it to the PS.

Our system model accounts for both computation and communication times. Both the PS and workers require time to perform model updates and gradient computations: these are represented in 6 as t_{COMP} (in 6, we show the computation time for W_2). Similarly, PS and workers require time to send messages. Although our simulator supports several communication primitives, in this work we restrict our attention to point-to-point communications. The time required to exchange messages is shown in 6 as t_{COMM} (in 6, we show the communication time for W_2). Intuitively, the “steeper” is the arrow representing a message exchange in the Figure, the faster is the communication.

Figure 6: Illustration of the distributed system operation. Example with one PS and 3 workers.



In our experiments, we generate computation and communication times according to samples from the following distributions. Computation times are drawn from *uniform distributions*, with a small support: we assume machines to be homogeneous in terms of computing times. Communication times are drawn from (truncated) *exponential distributions*: we assume the mass of communication times to be small, with some outlier message exchanges that take more time. Thus, $t_{\text{COMM}} \sim \lambda e^{-\lambda x}$.

The *rate* λ of the exponential is the parameter we vary in our experiments, to configure the system according to increasingly adverse asynchrony. Indeed, the above distributions, combined, determine the level of staleness the workers experience in the system. From 6, the staleness τ_t is defined as the difference between the current model iterate at the PS, and the last model iterate received by a worker and used to compute its stochastic gradient contribution. In the Figure, we show several values of τ_t , corresponding to stale gradient contributions to a more recent model iterate.

We use 5 to illustrate the staleness distribution for an entire simulation, that is, from the first model iterate, until a stopping criteria has been reached. Every time the PS receives a contribution from a worker, it increments the count in the bin corresponding to the staleness of the stochastic gradient message.

In the plots we show in 3, we summarize the staleness distribution using the rate of the exponential λ : a higher value is indicative of a system in which staleness induced by long communication delays is large.

C Simulator architecture overview

We believe important to present the general ideas behind the design of the simulator we use in our empirical study. Unfortunately, this is seldom the case in the literature, which hinders reproducibility. The source code of our simulator is open-source.³

The key conceptual design of our simulator is to separate concerns in different layers:

- The *low-level* layer implements the machinery of the simulator: it includes a process scheduler, message queues, and the management of virtual time. In this work, we use some of the low-level utilities from `PYTORCH-1.X` to manage processes. The low-level layer implements also the network abstraction, which allows point-to-point and broadcast primitives, as well as single or multi-socket interfaces.
- The *mid-level* layer focuses on stochastic optimization algorithms only. It uses two main abstract classes, one for the parameter server (PS) and one for the workers. Each variant of the SGD algorithm we use in our empirical validation inherits from such abstract classes and implement the specifics of each variation. The interface between the mid and low level layers allow the simulator to schedule processes for the parameter server and workers, as well as managing message exchange using queues.
- The *high-level* layer implements models, and provides utilities to read data. In this work, we use the `PYTORCH-1.X` library to describe models, and how they are trained. The interface between the high and low level layers allows exchanging model iterates, and gradients. Note that we use automatic differentiation from `PYTORCH-1.X` to compute gradients.

Since the simulator is multi-process, it can exploit multi-core architectures and can schedule worker processes to run on GPUs.

Overall, the above software design allows to: 1) easily introduce new models to study, as they can be readily imported from legacy `PYTORCH-1.X` code; 2) easily implement variants of stochastic optimization algorithms; 3) experiment with a variety of system configurations, including heterogeneity, various communication patterns, and various staleness distributions.

D Detailed experimental settings

General parameters

- Number of simulation runs per experimental setting: 5, with best parameters
- Number of workers = 8

³We will release the source code as an open repository after the review process ends.

- Network interface type: point-to-point, multi-socket
- $t_{\text{COMM}} \sim \text{Exp}(\lambda)$
- $\lambda = \{0.1, 1.0, 10.0\}$
- Truncation with offset = 0.002

KARDAM SGD specific paramters.

- Dampening function: exponential distribution $\sim \lambda e^{-\lambda\tau}$ with $\lambda = 0.2$

Models. All model parameters we used, including learning rates and momentum, are specified in Tables 1 and 2. Additional details are as follows.

- Target test accuracy = 91% (LENET), 70 % (RESNET-18)
- Training mini-batch size = 64
- Testing mini-batch size = 256

The CNN models are implemented in PYTORCH-1.X.

- LENET: architecture, $d = 61706$
- RESNET-18: architecture, $d = 11173962$

η	ϕ_{MEMSGD}	ϕ_{MEMSGD}	ASGD	KARDAM
LENET	0.002	0.002	0.002	0.005
RESNET-18	0.1	0.1	0.1	0.1

Table 1: Learning rate parameters.

momentum	ϕ_{MEMSGD}	ϕ_{MEMSGD}	ASGD	KARDAM
LENET	–	–	–	–
RESNET-18	0.9	0.9	0.9	0.9

Table 2: Momentum parameters.